https://doi.org/10.5194/wes-2021-148
Preprint. Discussion started: 23 December 2021

eawe european academy of wind energy
Open Access WIND ENERGY SCIENCE DISCUSSIONS

Model tests of a 10 MW semi-submersible floating wind turbine under waves and wind using hybrid method to integrate the rotor thrust and moments

Felipe Vittori[1], José Azcona[1], Irene Eguinoa[1], Oscar Pires[1], Alberto Rodríguez[2], Álex Morató[2], Carlos Garrido[2], and Cian Desmond[3]

[1]National Renewable Energy Centre (CENER), Dept. Wind turbine analysis and design, ciudad de la innovación, 7, Sarriguren (Navarra), 31621, Spain
[2]Saitec Offshore Technologies, Parque Empresarial Ibarrabarri, Edf. A2, 48940, Leioa-Bizkaia, Spain
[3]University College of Cork, Dep. Environmental Research Institute-MAREI, Haulbowline Road, Ringaskiddy, P43C573, Cork, Ireland

Correspondence: Felipe Vittori (fvittori@cener.com)

Abstract. This paper describes the results of a wave tank test campaign of a 1/49 scaled SATH 10 MW INNWIND floating platform. The Software-in-the-Loop (SiL) hybrid method was used to include the wind turbine thrust and the in-plane rotor moments $My - Mz$. Experimental results are compared with a numerical model developed in OpenFAST of the floating wind turbine. The tank test campaign was carried out in the scaled model tested at the Deep Ocean Basin from the Lir National Ocean TF at Cork, Ireland. This floating substructure design was adapted by Saitec to support the 10 MW INNWIND wind turbine within the ARCWIND project with the aim of withstanding the environmental conditions of the European Atlantic Area region. CENER provided the wind turbine controller specially designed for the SATH 10 MW configuration.

A description of the experimental set up, force actuator configuration and the numeric aerodynamic parameters are provided in this work. The most relevant experimental results under wind and wave loading are showed in time series and frequency domain. The influence of the submerged geometry variations in the pitch natural frequency is discussed. The paper shows the simulation of a case with rated wind speed, where the tilted geometry for the computation of the hydrostatic and hydrodynamic properties of the submerged substructure is considered. This case provides a better agreement of the pitch natural frequency with the experiments, than a equivalent simulation using the undisplaced geometry mesh for the computation of the hydrodynamic and hydrostatic properties.

1 Introduction

Floating wind energy has experienced a great technological development with the installation of the first floating wind farms.

A relevant contribution to this technological development is the ARCWIND project (Adaptation and Implementation of Floating Wind Energy Conversion Technology for the Atlantic Region), which is a European Union funded project that aims to foster renewable energies and energy efficiency. The general objective is to reduce the technical and economic uncertainties of floating wind technology to accelerate the up-scaling of the power capacity, making the large-scale floating projects more

https://doi.org/10.5194/wes-2021-148
Preprint. Discussion started: 23 December 2021

eawe european academy of wind energy
Open Access WIND ENERGY SCIENCE DISCUSSIONS

commercially attractive.

During this project the SATH floating platform, a single point mooring (SPM) floater developed by Saitec, was up-scaled to support the rotor-nacelle-assembly (RNA) of the wind turbine 10 MW INNWIND (Bak et al., 2013). The INNWIND tower was replaced by a design from Saitec. To study the technical feasibility of this floating wind turbine concept, a scaled tank test campaign was performed in the Lir National Ocean Test Facility at the University College Cork in Ireland.

Tank testing has been an important tool for the design of offshore floating structure (Chakrabarti, 2005), (Faltinsen, 1990), (Journée and Massie, 2001). In the case of innovative floating wind turbines, it is a critical step of the design to validate the platform dynamic response subjected to the complex interactions between the wind and wave loading. Moreover, tank testing allows validating and calibrating the hydro-aero-servo-elastic numerical tools that are used for the simulation and for the loads calculations used in the components structural design and certification of the system.

To achieve a reliable reproduction of the dynamics of the full scale floating offshore wind turbine (FOWT) in the basin, it is important to obtain an accurate scaling of the relevant forces acting on the system, the inertias and the frequencies of the time variant loads. The integration of the rotor dynamics in scaled tests that combine wind and wave loading is challenging due to the scaling conflict between the Reynolds and Froude numbers that govern the aerodynamic and hydrodynamic forces (Bredmose et al., 2012) (Azcona et al., 2014b).

A hybrid testing approach named Software-in-the-Loop (SiL) was proposed and successfully applied in a test campaign by Azcona et al. (2014). In this method, the aerodynamic rotor thrust of the wind turbine is applied to the scaled model by a ducted fan or a set of propellers. The turbine thrust force is based on real-time simulations at full scale of the rotor aerodynamics, coupled with the scaled floater response that is physically tested under wave loading. The method allows considering the correctly scaled rotor load in the wave tank tests. Moreover, as the rotor loading is coupled in real time with the floater motion, the aerodynamic damping introduced by the rotor is captured. This effect is a relevant source of damping and cannot be neglected in order to accurately capture the global motions of the floating turbine. Similar methods have been applied more recently, for example by Bachynski, Chavaud, and Sauder (2015) and Belloli et al. (2020). Also, there are different approaches to introduce an aerodynamic thrust representing the full scale rotor force, such as using a drag disk Roddier et al. (2010) or building a Froude scaled rotor Koch et al. (2016).

The first version of the SiL method, where just the rotor thrust force is introduced, was successfully applied in several test campaigns for floating wind turbines. For example, in Vittori et al. (2018) the experimental measurements using this first version of SiL were compared with results from numerical computations showing good agreement and in Azcona et al. (2019) the method showed its capability to capture the low frequency dynamics of a semi-submersible. Afterwards, the SiL method was expanded to also include rotor aerodynamic and gyroscopic moments for the pitch (M_y) and the yaw (M_z) platform degrees

https://doi.org/10.5194/wes-2021-148
Preprint. Discussion started: 23 December 2021

eawe european academy of wind energy
Open Access WIND ENERGY SCIENCE DISCUSSIONS

of freedom (DoF). This improved SiL method was used in Vittori et al. (2020) and Fontanella et al. (2020), and is also applied in this test campaign.

This paper shows how the SiL method, including rotor moments, is able to reproduce the dynamic response of the SATH 10MW INNWIND (SATH10MW) floating offshore wind turbine. The measurements from experiments are compared with the numerical simulations of equivalent cases using OpenFAST (NREL, 2019) and the results are discussed.

The first section of this works gives an overview about SiL methodology applied in this test campaign, the scaled model of the SATH10MW and the campaign setup. The second section presents a description of the OpenFAST numerical model for the SATH10MW floating wind turbine. Finally, the analysis of the results is presented in the third section, ending with the conclusions of this work.

2 Description of the Software-in-the-loop methodology (SiL)

The SiL hybrid method consists of replacing the rotor by a force actuator (a fan or a multipropeller system) driven by an electric motor. The scaled thrust is controlled by the motor rotational speed set by an electronic controller, which again depends on the real time simulation of the full scale rotor in a turbulent wind field, considering turbine control action with the platform motions measured in real time in the wave tank test. The FAST code developed by NREL (Jonkman , 2007) is used for the simulation of the rotor thrust loads. The details on the SiL system architecture can be in found in Azcona et al. (2014).
In this test campaign, an actuator with 4 propellers was used to introduce the rotor loading. A photograph of this actuator in the calibration workbench is shown in Fig. 1.

Each of the propellers is powered by a drone commercial brushless motor that is controlled by an Electronic Speed Controller (ESC), and fed with an industrial AC/DC power supply. This system configuration produces an approximate force range of 0-24 N. The rotational speed of each motor (and therefore the force produced by the propeller) is controlled by a Pulse Width Modulation (PWM) signal that is generated with the LabVIEW control software, using servo libraries for Arduino. Figure 2 shows a diagram of the SiL system control scheme.
The measured motions from the tracking system of the wave tank are acquired by the SiL control scripts in LabVIEW, and then are integrated the simulation software for the computation of the rotor loads. This demanded rotor loading is transformed into the different propeller signals through force and moment balance equations. The propellers can work introducing only the thrust force of the rotor (each of the propellers introduces 1/4 of the scaled thrust), or the system can decouple the force that each propeller introduces, to generate the required pitch (M_y) and yaw (M_z) moments, together with the thrust. This enables the system to reproduce the scaled rotor moments from aerodynamic effects such as imbalance, wind shear, pitch failures, wind misalignment and gyroscopic effects. In this test campaign, the moments M_y and M_z were included in the test. The details

https://doi.org/10.5194/wes-2021-148
Preprint. Discussion started: 23 December 2021

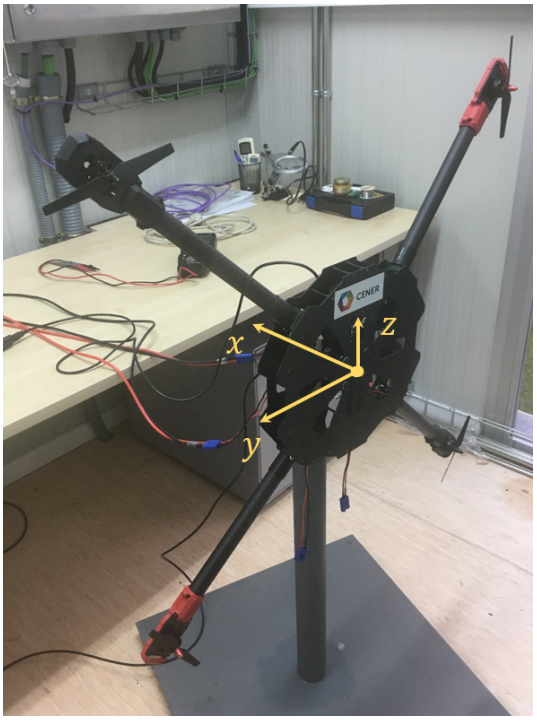

Figure 1. Multi-propeller actuator at CENER calibration workbench. Wind turbine thrust is applied in the x direction, rotor moment M_y and M_z is applied in the y and z axis, respectively.

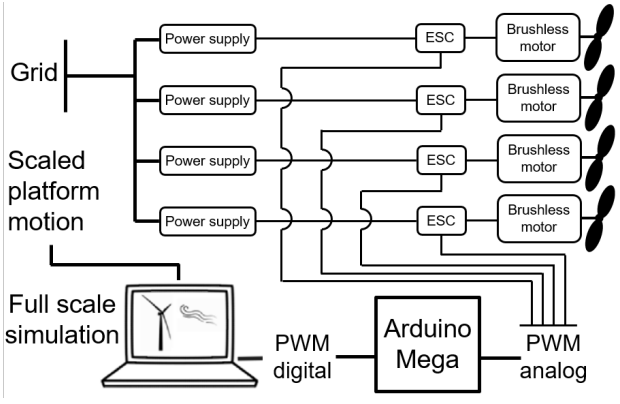

Figure 2. SiL control diagram. (Vittori et al., 2020)

about the development of this multi-propeller actuator can be found in Pires et al. (2020).

90

https://doi.org/10.5194/wes-2021-148
Preprint. Discussion started: 23 December 2021

eawe european academy of wind energy
Open Access WIND ENERGY SCIENCE DISCUSSIONS

2.1 Rotor loading hybrid numerical model

A numerical model of the 10 MW INNWIND rotor was built at full scale using the FAST code coupled with AeroDyn 12.58 (Jonkman , 2007). For the execution of the experiments, it was used a modified version of this software Azcona et al. (2014) able run in real time and to integrate the measured platform motions in the computation of the rotor loads. The aerodynamic loads are based in Blade Element Momentum (BEM) model using the Glauert correction. The tip and hub losses were considered using the Prandtl correction. The blades and the tower were considered rigid. The turbulent wind was obtained through a Kaimal spectrum using the TurbSim wind generator from NREL (Jonkman , 2016).

The turbine controller used for the experiments was developed by CENER on the basis of state-of-the-art control strategies for pitch-controlled variable-speed turbines. Collective pitch-to-feather was applied through gain-scheduled PID controller in the above rated region, where a constant power strategy was implemented.

2.2 SATH 10MW scaled tank testing

The 1/49 SATH10MW scaled floating platform is shown in Fig. 3. This floater concept has a low draft and has a SPM configuration that allows it to freely rotate. The SPM system was not implemented in the scaled model and, instead, a retention system based on 4 horizontal lines separated by 90 deg between them was used to moor the system as is shown in Fig. 3.

The drone frame with the four propellers that are used to introduce the scaled 10 MW INNWIND rotor loads was installed at the tower top of the scaled floating platform. The reference system for the loads is indicated at the tower top in Fig. 3. The water depth at full scale is 110 m and the wave generator produces waves in the direction also indicated in Figure 3.

The results presented in this work are based on a coordinate system located at the intersection of the MSL (Mean Sea Level) and the tower axis indicated in Fig. 3 in red color. The geometrical center of the drone frame was located at the equivalent full scale hub height of the wind turbine.

The resulting mass of the set of propellers together with the carbon fiber arms and the frame was relatively low, and thus ballast was added in order to match the target weight that represents the full scale 10 MW INNWIND RNA mass.

3 SATH10MW OpenFAST numerical model for comparison

A numerical model of the SATH10MW was built at full scale in OpenFAST v2.2 (NREL, 2019) with the objective of reproducing numerically the experimental cases and compare the results with the experimental measurements. The platform added mass, damping, hydrostatic stiffness and wave force coefficients were obtained from the potential theory WAMIT (Lee and Newman , 2006) code in frequency domain and then, given as an input to OpenFAST. For the simulation of the experimental cases, the measured wave elevation time series from the tests were used as an input to OpenFAST, which generates the wave kinematics with first order wave theory.

https://doi.org/10.5194/wes-2021-148
Preprint. Discussion started: 23 December 2021

eawe european academy of wind energy
Open Access WIND ENERGY SCIENCE DISCUSSIONS

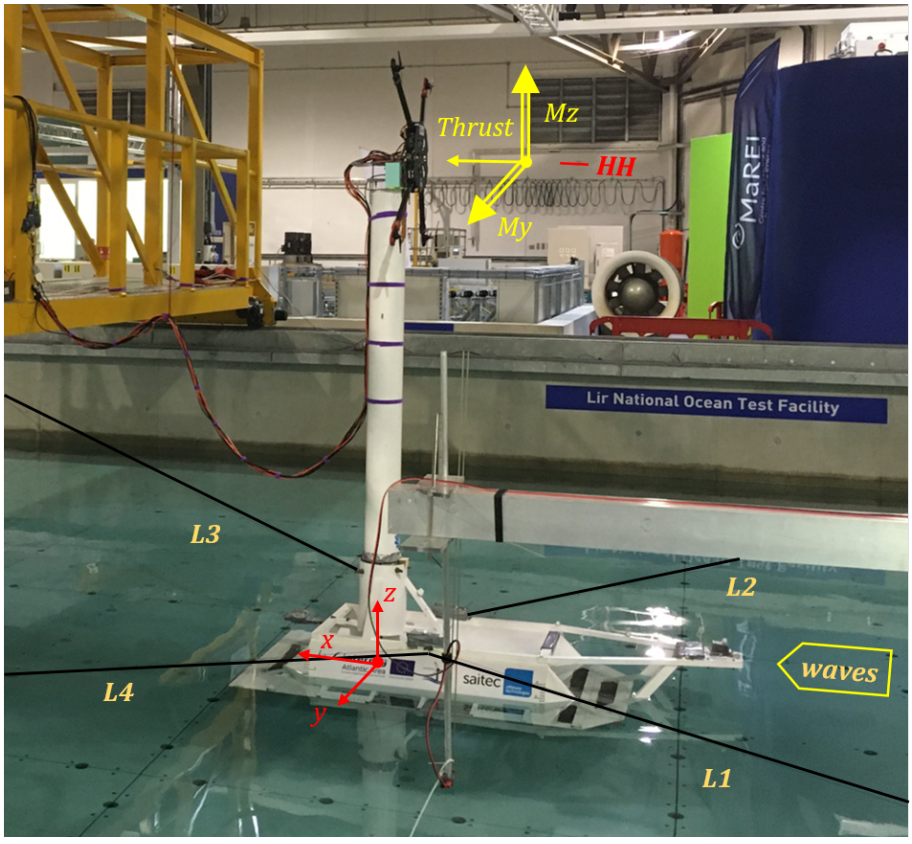

Figure 3. SATH10MW scaled model.

The second order hydrodynamic forces was implemented by means of Newman approximation. Saitec provided inputs files to be used in OpenFAST. Additional linear and quadratic damping coefficients were incorporated in all platform DoF after the model damping was calibrated based on the experimental decay tests.

The horizontal mooring system of the scaled floater was modeled using a linear stiffness matrix, considering the couplings between the corresponding DoF.

The aerodynamic loads were calculated with AeroDyn v15, through the Blade Element Momentum (BEM) model using the Glauert correction. The tip and hub losses were considered using the Prandtl correction. This model was defined with tower and blades rigid to match the experiment conditions. The input wind field used in the simulations were the same used during the experiments to maintain consistency. Finally, the same wind turbine controller used during the tank testing was used in the numerical model.

https://doi.org/10.5194/wes-2021-148
Preprint. Discussion started: 23 December 2021

eawe european academy of wind energy
Open Access WIND ENERGY SCIENCE DISCUSSIONS

4 Results discussions

This section presents some of the most relevant experimental measurement together with the numeric results obtained from the calibrated numerical model simulated by OpenFAST. The next load cases presented start with the more simple tests like free decay until the validation of more complex load scenarios like simultaneous turbulent wind and irregular waves. This allows isolating the different effects to simplify the analysis as it was also recommended by Robertson et al. (2013).

First, it is shown the results from the free decay tests, that were used to calibrate the numerical model. These results show that the platform natural frequencies and damping levels are similar to the full scale numeric model in OpenFAST.

Second, it is presented the platform response under constant and uniform wind using SiL method to introduce the rotor loads. Through these tests it was verified that the rotor loads produced a similar displacement in the experiment than the full scale numeric model.

Finally, it is presented the similarity obtained between numerical results and measurements when the platform is under turbulent wind only. Additionally, the effect of the new SiL is shown when the floating platform is under wave and wind loading. All results presented in this document are at full scale.

4.1 Free decay tests

The free decay experimental results allowed calibrating the hydrodynamic damping levels of the OpenFAST SATH10MW model adjusting the linear and quadratic damping terms. Also, the natural periods of the platform DoF were obtained by adjusting the coefficients of the stiffness matrix for the mooring system. In these experimental tests the SiL actuator was turned off. Figure 4 (a) and (b) show the good agreement found by the OpenFAST model for surge and sway, respectively. Figure 5 (a) and (b) shows the good approximation obtained for pitch and yaw respectively.

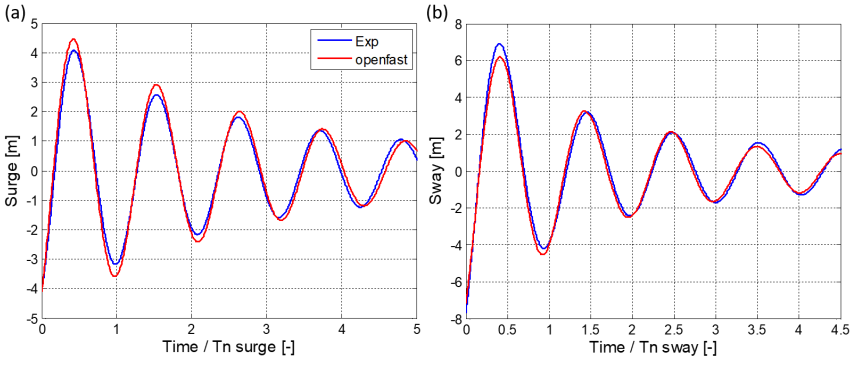

Figure 4. Free decay results for (a) surge and (b) sway

It has to be mentioned that in the experiment it was observed the influence of the cable bundle of the actuator in the platform position and stiffness. This effect was taken into account during the pitch calibration of the numeric model of OpenFAST and

https://doi.org/10.5194/wes-2021-148
Preprint. Discussion started: 23 December 2021

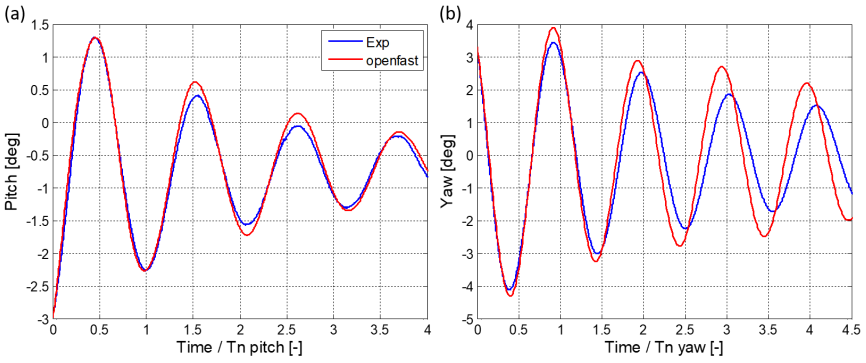

Figure 5. Free decay results for (a) pitch and (b) yaw

155 produces a 3% of difference with respect the platform stiffness not considering these cables. Also, the pitch mean position was affected by the cables.

A good agreement is also obtained between numerical model and experiment in the yaw DoF. Obviously, an SPM system would not produce any restriction in yaw allowing to freely rotate.

160

The values of the natural periods are not shown due to confidential restrictions. The surge and sway results from Fig. 4 (a) and (a) are referred to the center of mass of the floating wind turbine to make easier the interpretation of the DoF response. There is strong coupling between certain DoF, such as sway and yaw when using the coordinate system from Fig. 3.

165 For the following sections, the results will be referred to the coordinated system indicated in Fig. 3.

4.2 Constant and uniform winds only

Figure 6 presents the steady state response comparison for the platform surge and pitch displacements between experimental measurements and numerical results. There are no wave and the wind is constant and uniform. The openFAST results were very close to the experiments for 7.5 m/s case the differences between them were below 1% for surge and pitch. In the case of 170 11.4 m/s of wind speed the numerical result for surge was 5% larger than the experiment. The simulation solution for pitch was 2% below the tank test at turbine rated wind speed of 11.4 m/s.

The good agreement between numerical results and experimental measurements for the surge and pitch responses under both wind speeds indicates the equivalence between the scaled experimental model and the numerical model .

https://doi.org/10.5194/wes-2021-148
Preprint. Discussion started: 23 December 2021

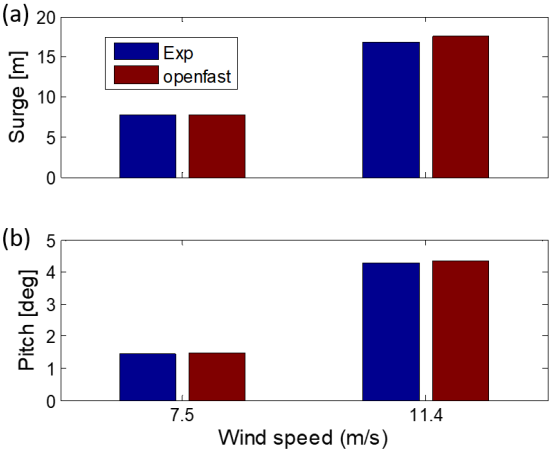

Figure 6. Steady state response comparison between experiments (improved SiL) and OpenFAST simulation for (a) Surge and (b) Pitch response

4.3 Turbulent winds only

In this section, the motions of the platform under a turbulent wind loading, with no waves, are discussed. Figure 7 shows the comparison between the measurements in the experiment and the computations from the equivalent simulations in OpenFAST for the platform surge and pitch motions, under a 7.5 m/s turbulent mean wind speed. Results are presented in time domain and in frequency domain, with a Power Spectral Density (PSD).

Time domain surge response from OpenFAST in Fig. 7 (a) matches well the response measured in the experiment. The surge Power Spectrum Density (PSD) Fig. 7 (b) also shows the agreement between numerical and experiment results in the lower frequencies region and around the surge natural frequency, indicated in the plot.

In the case of the SATH10MW pitch response in Fig. 7 (c) the simulation results and measurements agree well for the the lower frequencies, were the wind energy is located, but for the higher frequencies, around platform pitch natural frequency, the motion is underestimated by the simulations.

Figure 8 (a) and (b) shows that there is significant difference between the measured and calculated sway response. The sway response in the experiments has larger excursions than the calculated in the numeric simulations. Additionally, the sway natural period of the scaled model seems to be slightly shifted with respect to the numerical model.
The yaw response comparison in Fig. 8 (c) shows a certain agreement between the measured scaled motion and the simulation results, although the OpenFAST solution presents lower peaks for the yaw rotations. This can be also observed in the yaw PSD

https://doi.org/10.5194/wes-2021-148
Preprint. Discussion started: 23 December 2021

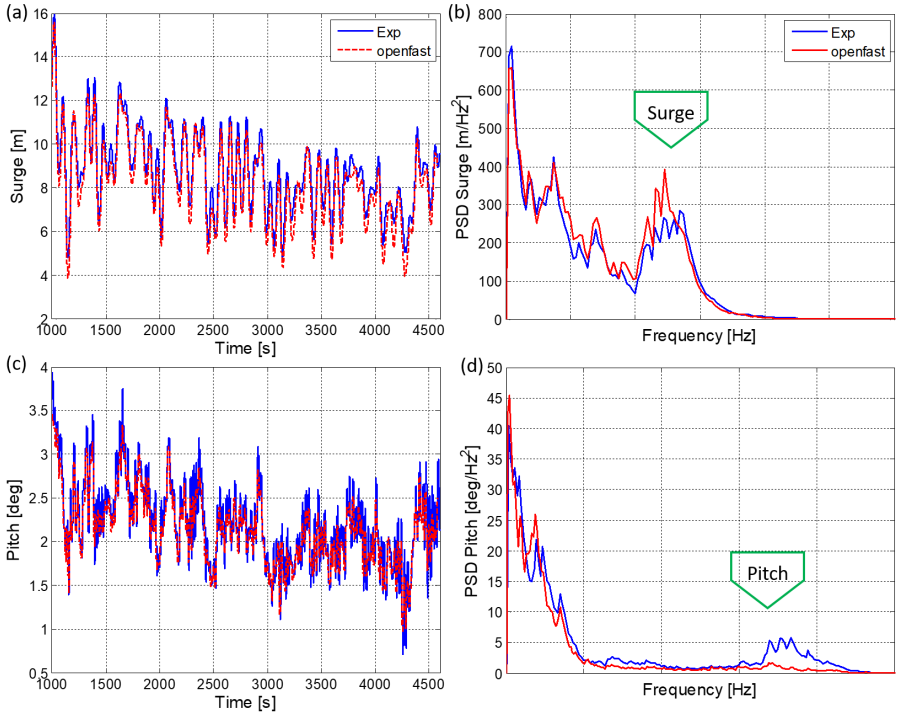

Figure 7. Platform response comparison between experiments and OpenFAST simulation for surge and pitch under 7.5 m/s turbulent mean wind speed without waves. (a) Surge response in time domain (b) Surge response PSD (c) Pitch response in time domain and (d) Pitch response PSD

Fig. 8 (d) where the simulation curve presents lower values than the experimental.

4.4 Turbulent winds and irregular waves

This section compares the experimental measurements and the numerical simulations for two cases with combined turbulent wind and irregular waves. The first case has a mean wind speed of 7.5 m/s with co-linear irregular waves with $H_s =$ 2.0 m and $T_p = 8.5$ s. The second case has a mean speed of 11.4 m/s with co-linear irregular waves with $H_s =$ 3.0 m and $T_p = 10.5$ s.

Two different numerical simulations are plotted against the experiments in this section. One of the simulations applies linear potential hydrodynamics ($openfast\ hyd: 1st$). The other one includes second order effects using the Newman approximation ($openfast\ hyd: 1st + 2nd$). For both, experiment and simulation results, it was used the same turbulent wind field, wave elevation time series and wind turbine controller.

Figure 9 and Fig. 10 shows the measured and simulated platform surge for the turbulent wind speed of 7.5 m/s and 11.4 m/s with their respective wave conditions. It can be seen that the numerical simulations are very close to the experimental response for both environmental conditions. Also, it can be noticed that the non linear hydrodynamics provides a certain improvement

https://doi.org/10.5194/wes-2021-148
Preprint. Discussion started: 23 December 2021

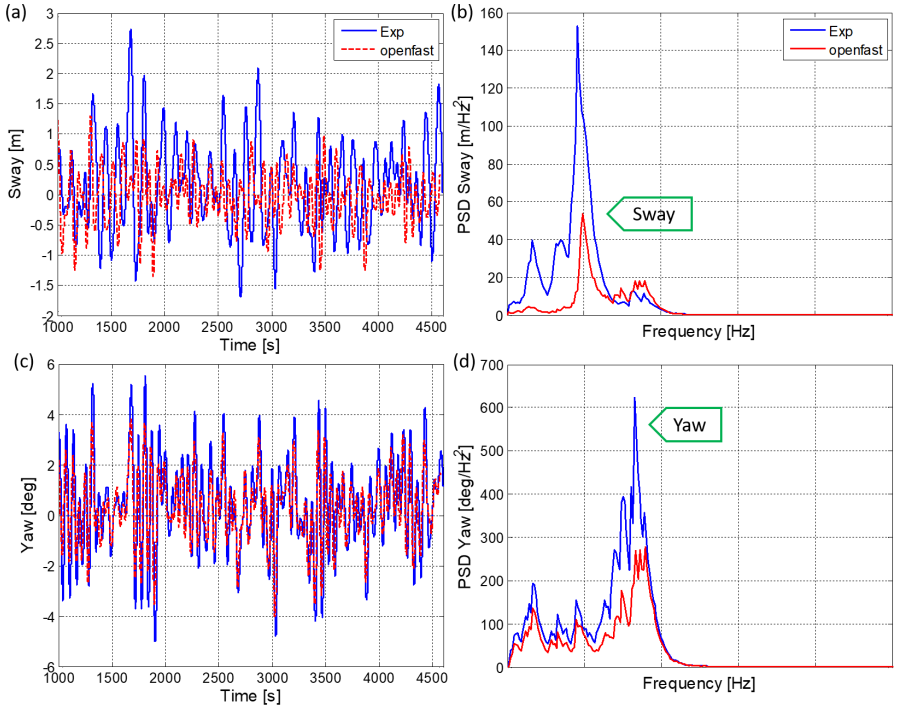

Figure 8. Platform response comparison between experiments and computations of sway and yaw under 7.5 m/s turbulent mean wind speed without waves. (a) Sway response in time domain (b) Sway response PSD (c) Yaw response in time domain and (d) Yaw response PSD

in the numeric prediction as it can be seen between 6500 s and 7000 s in Fig. 9. In the case of 11.4 m/s Fig. 10 both numerical solutions are very similar, probably because the platform motions is dominated by the wind load. Similar results on the effect of second order hydrodynamics in the response of the platform were observed by Azcona et al. (2019) and Roald et al. (2013).

The PSD of the surge responses for the experiments at 7.5 m/s and 11.4 m/s is presented in Fig. 11 (a) and (b) respectively. On both figures (a) and (b) the maximum energy is located at the platform surge natural frequency. This natural frequency is excited by low frequency loads such as the wind loading and the wave second order difference-frequency effects.

Fig. 11 (a) and (b) shows that the numerical platform surge motion with first order hydrodynamic is very similar to the experimental curve in the low frequency region. This indicates that with the wind and wave conditions tested the second order hydrodynamics is not contributing significantly to the platform response. This also mean that the wind turbine loading is dominating the response for both wind speed. This was also reported in Azcona et al. (2019) for the OC4 platform with the 5MW NREL wind turbine, where the wind loading dominates the platform response compared to hydrodynamics near rated wind speed.

Both PSD present a sudden decrease of the surge response inside the wave frequency region. This is a cancellation effect and is the result of the interaction of the length of the floater with the incident wave length that produce no force and moment on

https://doi.org/10.5194/wes-2021-148
Preprint. Discussion started: 23 December 2021

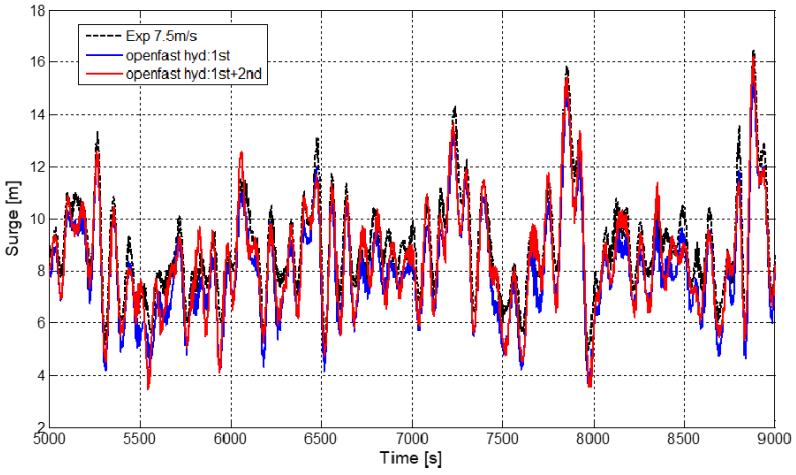

Figure 9. Time series for platform surge response under 7.5 m/s turbulent mean wind speed and irregular waves $H_s = 2.0$ m; $T_p = 8.5$ s

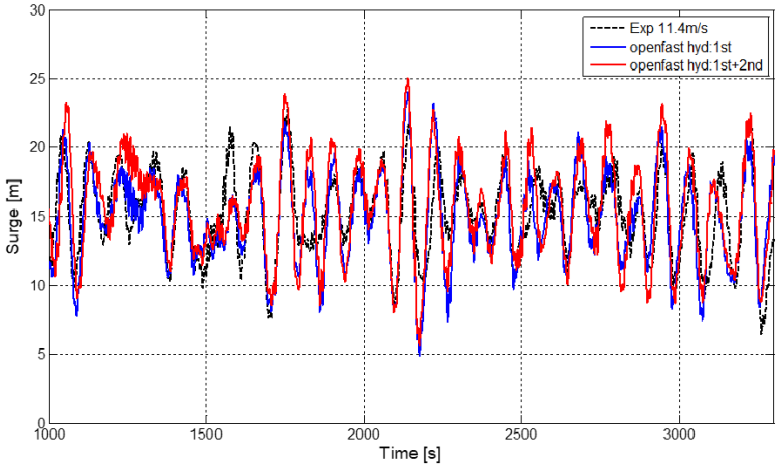

Figure 10. Time series for platform surge response under 11.4 m/s turbulent mean wind speed and irregular waves $H_s = 3.0$ m; $T_p = 10.5$ s

the SATH platform at a particular cancellation frequency. This cancellation effect is indicated in Fig. 11 (b).

The platform PSD pitch response for 7.5 m/s is presented in Fig. 12 (a). Both numerical models approach well the experimental response, but at the pitch natural frequency the numerical models underestimate the experimental peak.

The pitch response for the mean wind speed of 11.4 m/s is shown in Fig.12 (b). This PSD shows that the experimental pitch natural frequency is shifted to a lower frequency with respect to the value obtained from the free decay test and also with respect to the experiment for 7.5 m/s in Fig. 12 (a). The numerical results does not present this displacement to a lower frequency

https://doi.org/10.5194/wes-2021-148
Preprint. Discussion started: 23 December 2021

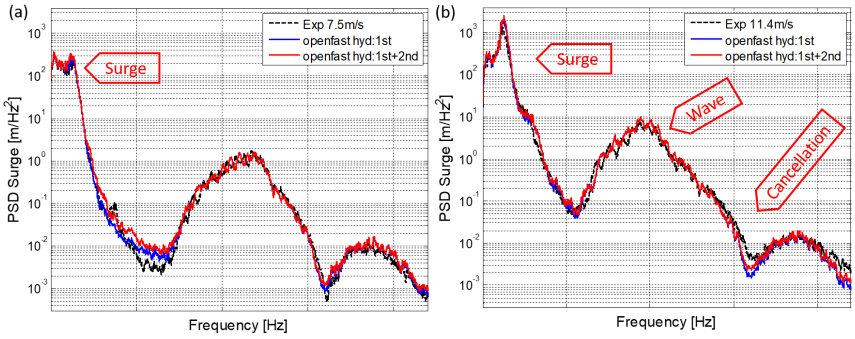

Figure 11. Surge PSD response of SATH10MW under (a) turbulent wind with average of 7.5 m/s and irregular waves $H_s = 2.0$ m; $T_p = 8.5$ s and (b) turbulent wind with average of 11.4 m/s and irregular waves $H_s = 3.0$ m; $T_p = 10.5$ s

of the natural frequency, and the result is coherent with the natural frequency at the experiment for 7.5 m/s in Fig. 12 (a). The reason for this decrease in the experimental pitch natural frequency will be discussed in detail in the next section.

Figure 13 and Fig. 14 show that the platform yaw response predicted by the numerical simulation for the two turbulent wind speed match with very good agreement the experimental yaw response in time domain. This also indicates that the rotor moment around the vertical axis, M_z, introduced by the actuator in the experiment is correctly captured.

4.5 Hydrodynamic modeling of a floating platform in openFAST

As it was discussed in the previous section, in relation with in Fig. 12 (b) the platform pitch natural frequency in the experiment is shifted to a lower frequency, in comparison with the natural frequency observed in the free decays and in the PSD's for the cases with 7.5 m/s of turbulent mean wind speed.

This shift in the natural frequency could be caused by the change on the hydrostatic and hydrodynamic properties of the submerged substructure due to the pitch rotation of the platform at rated wind speed. In this case, the platform presents a mean pitch inclination of 4.3 deg and mean heave of -1.2 m.

To confirm this hypotheses, we built a new mesh of the submerged substructure for the geometry corresponding to the pitched platform at rated wind speed. Figure 15 (a) present the mesh for the original geometry of the submerged platform, used in WAMIT to calculate the added mass, potential damping, hydrostatic stiffness and wave excitation coefficients.

Figure 15 (b) present the mesh for the submerged substructure geometry corresponding to the mean pitch and heave at 11.4 m/s turbulent mean wind speed. It is equivalent to the platform position observed during the experiments as in Fig. 15 (c).

The new tilted geometry from Fig. 15 (b) produced a reduction in the hydrostatic stiffness for the pitch DoF of around 2%. The case with turbulent wind at rated wind speed of 11.4 m/s and irregular waves was simulated again with the new hydrostatic and hydrodynamic properties computed for the tilted geometry. The results are compared with the original simulation and

https://doi.org/10.5194/wes-2021-148
Preprint. Discussion started: 23 December 2021

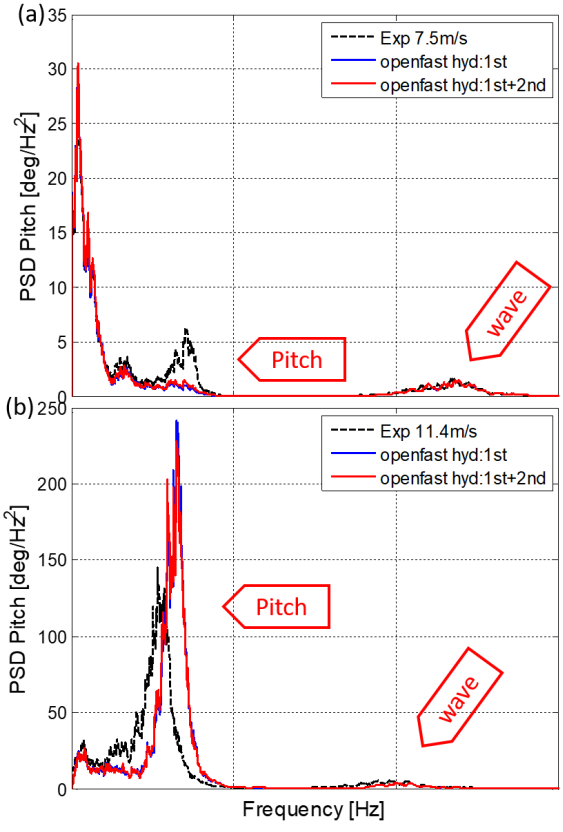

Figure 12. Pitch PSD response of SATH10MW under turbulent wind with average of (a) 7.5 m/s and irregular waves $H_s = 2.0$ m; $T_p = 8.5$ s and (b) 11.4 m/s and irregular waves $H_s = 3.0$ m; $T_p = 10.5$ s

with the experiments in the pitch PSD in Fig. 16. This plot shows that the natural frequency of numerical results with the tilted geometry also decreases with respect to the original simulation where the mesh is not pitched. The new frequency now matches the shifted pitch frequency from the experiments. This indicates that the advanced shape of this platform requires a careful consideration of the geometrical non-linearities to obtain accurate numerical results.

The pitch response at the wave frequency remained similar when the platform is tilted. Also, the surge response with the tilted geometry result was not different compared to the non-tilted geometry in the wave frequency region. The added mass in yaw increased a 14% with the tilted geometry, but it did not impact the platform yaw response.

https://doi.org/10.5194/wes-2021-148
Preprint. Discussion started: 23 December 2021

eawe european academy of wind energy
Open Access WIND ENERGY SCIENCE DISCUSSIONS

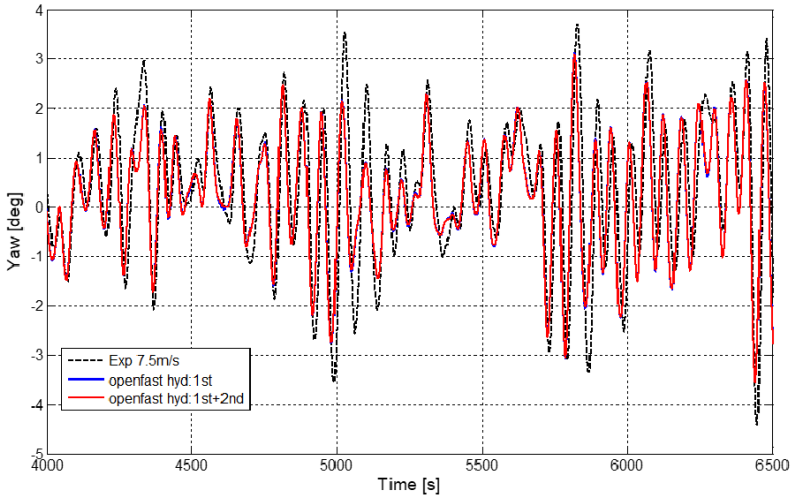

Figure 13. Yaw response of SATH10MW under turbulent wind with average of 7.5 m/s and irregular waves $H_s = 2.0$ m; $T_p = 8.5$ s

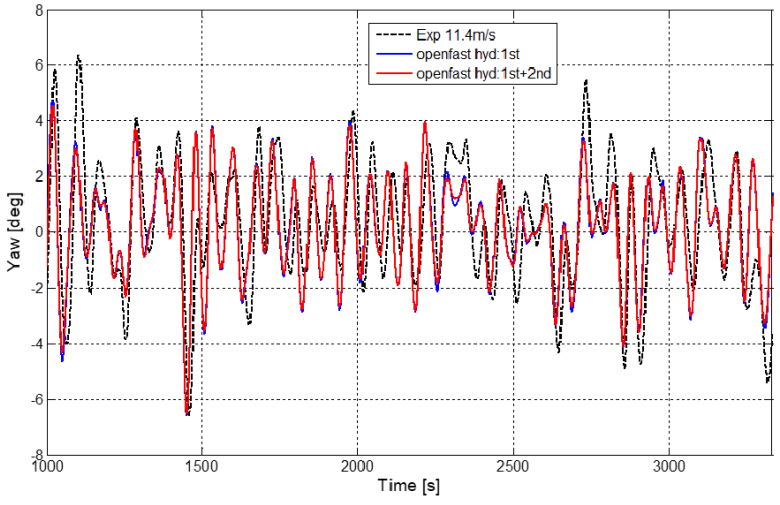

Figure 14. Yaw response of SATH10MW under turbulent wind with average of 11.4 m/s and irregular waves $H_s = 3.0$ m; $T_p = 10.5$ s

5 Conclusions

The hybrid SiL methodology was applied to a tank test campaign of the floating offshore substructure SATH supporting the INNWIND 10 MW wind turbine, which was performed at the Lir national Ocean Test Facility of UCC.

https://doi.org/10.5194/wes-2021-148
Preprint. Discussion started: 23 December 2021

eawe european academy of wind energy
Open Access WIND ENERGY SCIENCE DISCUSSIONS

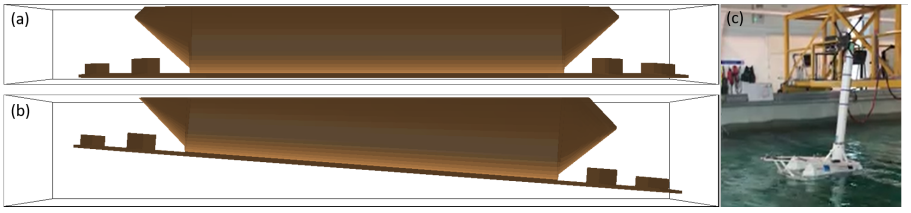

Figure 15. (a) Geometry of the wet surface of the platform at its equilibrium position. (b) Geometry of the wet surface of the platform considering the platform mean pitch and heave displacements under a turbulent wind of 11.4 m/s of mean wind speed and irregular wave. (c) Photograph of the platform during tank testing under wind and wave loading

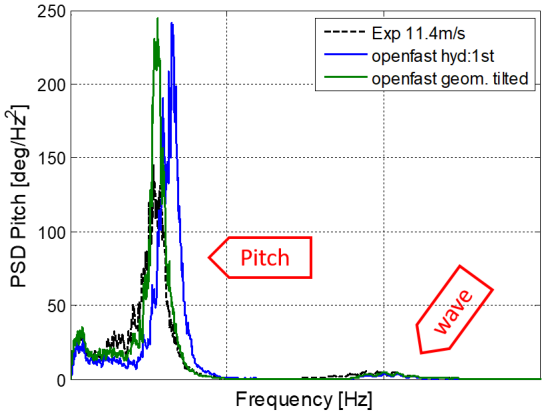

Figure 16. Pitch PSD response comparison between experiment curve, numeric model with platform without tilt and tilted under turbulent wind 11.4 m/s and irregular waves $H_s = 3.0$ m; $T_p = 10.5$ s

During the experimental campaign it was used the more recent version of the SiL method that is able to introduce the rotor thrust and also the moments in the yaw and pitch axes.

The experimental results were used for the calibration of a numerical model in OpenFAST of the SATH10MW floating wind turbine, and later used to compare the measurements with respect the simulation results.

The constant and uniform wind only tests confirmed that the simulations and experiments are in agreement for the static platform response and the loading exerted by the SiL actuator. The largest difference obtained between numerical and measurements was 5% for surge response at 11.4 m/s of wind speed.

The turbulent wind only case showed a very good agreement between computations and experiments, including the yaw DoF. This demonstrates the capability of the new SiL for including simultaneously the wind turbine thrust and the rotor moments on

https://doi.org/10.5194/wes-2021-148
Preprint. Discussion started: 23 December 2021

the scaled floating platform, also including the effect of the control strategy, aerodynamic damping and wind turbulence.

Platform surge response under turbulent wind and irregular wave was predicted well by the OpenFAST model. The wind turbine aerodynamic loading dominates the platform response under the wind and wave condition tested for the low frequencies. The second order hydrodynamics introduced with the Newman approximation in the simulations did not produced a significant improvement of the numerical prediction for the conditions tested.

The platform pitch response obtained by openFAST was similar to the measured in the experiments for the lower wind speed. However, it was observed that for the case at rated wind speed, where the platform presents a relevant mean pitch, important non-linear geometrical effects arise that affect the pitch natural frequency. For this case, the simulation considering the hydrodynamic and hydrostatic properties of the tilted submerged geometry provided a good agreement between the pitch natural frequency of the experiment and the updated numerical model.

The experimental yaw response of the platform matched well the numerical solution. The version of SiL including the moment in the yaw axis captured well the platform rotations for this degree of freedom.

Author contributions. FV reviewed the experimental data contributing to the results analysis, validation and calibrated the numerical model in OpenFAST. JA contributed in the conceptualization of the work, the experimental and validation results analysis, the preparation of the SiL hybrid numerical model and revision of the paper. OP supervised the SiL operation during tests at the tank and defined the actuator control system and improve the interface in LabVIEW of the SiL control program. IE developed the wind turbine controller for the SATH10MW INNWIND floating wind turbine. AR was responsible of the experiment tests and helped to define each tests of the experimental campaign. AM contribute in the definition of the experiment tests and model scales. CG was supervising the preparation activities before the test campaign. CD was responsible of the tank instrument and operation of the wave generator, also helped to define the test methodology. FV prepared the manuscript of this article with contribution from all co-authors

Competing interests. Authors declares that they have no conflict of interest

Acknowledgements. This test campaign and the results presented were developed within the project ARCWIND – Adaptation and implementation of floating wind energy conversion technology for the Atlantic region, which is co-financed by the Interreg Atlantic Area Programme through the European Regional Development Fund under contract EAPA 344/2016. Authors want also to give thanks for their assistance during the experiments set up to Christian van den Bosch and Otter Aldert from University College of Cork. Also, authors want to thanks

https://doi.org/10.5194/wes-2021-148
Preprint. Discussion started: 23 December 2021

Juan Martínez Belio and Jon Olagüe from the Structural Area of Dept. Wind turbine analysis and design (CENER) for his support on the mesh generation from the CAD floating platform.

https://doi.org/10.5194/wes-2021-148
Preprint. Discussion started: 23 December 2021

eawe european academy of wind energy
Open Access WIND ENERGY SCIENCE DISCUSSIONS

References

Azcona J., Bouchotrouch F., González M., Garciandía J., Munduate X., Kelberlau F. and Nygaard T.A. (2014) "Aerodynamic Thrust Modelling in Wave Tank Tests of Offshore Floating Wind Turbines Using a Ducted Fan. Fan." Journal of Physics: Conference Series Vol. 524 DOI 10.1088/17426596/524/1/012089

Azcona J., Bredmose H., Campagnolo F., Manjock A., Pereira R. and Sander F. (2014) INNWIND D4.22: Verification and Validation of design methods for floating structures

Azcona J., Bouchotrouch F. and Vittori F., (2019) "Low-frequency dynamics of a floating wind turbine in wave tank–scaled experiments with SiL hybrid method", Wind Energy, Vol. 22, Issue10. DOI: 10.1002/we2377.

Bachynski E., Chavaud V., and Sauder T. (2015) "Real Time Hybrid Model Testing of Floating Wind Turbines: Sensitivity to Limited Actuation" 12th Deep Sea Offshore Wind R&D Conference, EERA DeepWind. vol. 80, pp. 2 12, Trondheim, Norway.

Bak, C., Zahle, F., Bitsche, R., Taeseong, K., Yde, A., Henrik-sen, L. C., Natarajan, A., & Hansen, M. H. 2013 "Descrip-tion of the DTU 10 MW Reference Wind Turbine" Technical Report Report-I-0092 DTU Wind Energy.

Belloli M., Bayati I., Facchinetti A., Fontanella A., Giberti H., La Mura F., Taruffi F. and Zasso A. (2020) A hybrid methodology for wind tunnel testing of floating offshore wind turbines, Ocean Engineering, 210, https://doi.org/10.1016/j.oceaneng.2020.107592

Bredmose H., Larsen S. E., Matha D., Rettenmeier A., Marino E. and Saettran L. 2012 MARINET D2.4: Collation of offshore wind wave dynamics

Chakrabarti S.K. (2005) Handbook of Offshore Engineering (Vol. 2). Elsevier

Faltinsen O.M. (1990) Sea Loads on Ships and Offshore Structures. Cambridge University Press

Fontanella A., Liu Y., Azcona J., Pires O., Bayati I., Gueydon S., de Ridder E. J., van Wingerden J. W. and Belloli M. (2020) A hardware-in-the-loop wave-basin scale-model experiment for the validation of control strategies for floating offshore wind turbines, Journal of Physics Conference Series, vol. 1618.

Jonkman J. M. (2007) Dynamics Modeling and Loads Analysis of an Offshore Floating Wind Turbine, Technical Report NREL/TP-500-41958

Jonkman B. (2016) TurbSim user's guide: version 2.0. Draft Report, Boulder, CO, USA, NREL.

Journée J.M.J and Massie W.W (2001) Offshore Hydromechanics. (1st edition) Delft University of Technology

Koch C., Lemmer F., Borisade F., Matha D., and Cheng P. W. (2016) "Validation of INNWIND.EU Scaled Model Tests of a Semisu bmersible Floating Wind Turbine. Proceedings of the Twenty sixth International Conference on Offshore and Polar Engineering, Rhodes, Greece. URL http://dx.doi.org/10.18419/opus 8967

Lee C. H. and Newman J. N. 2006 WAMIT® User Manual, Versions 6.3, 6.3PC, 6.3S, 6.3S-PC, Chestnut Hill, MA: WAMIT, Inc.

NREL (2019) OpenFAST v2.2. Retrieved from https://github.com/OpenFAST/OpenFAST/tree/v2.2.0

Pires O., Azcona J., Vittori F., Bayati I., Gueydon S., Fontanella A., Liu Y., de Ridder E.J., Belloli M., van Wingerden J.W. (2020) Inclusion of rotor moments in scaled wave tank test of a floating wind turbine using SiL hybrid method Journal of Physics: Conference Series 1618 032048 doi 10.1088/1742-6596/1618/3/032048

Robertson A., Jonkman J., Masciola M., Molta P., Goupee A., Coulling J., Prowell I. and Browning J. (2013) "Summary of Conclusions and Recommendations Drawn from the DeepCWind Scaled Floating Offshore Wind System Test Campaign", 32nd International Conference on Ocean, Offshore and Arctic Engineering OMAE, Nantes, France.

https://doi.org/10.5194/wes-2021-148
Preprint. Discussion started: 23 December 2021

Roald L., Jonkman J., Robertson A. and Chokani N. (2010) "The effect of second-order hydrodynamics on floating offshore wind turbines" Energy Procedia 35 253 - 264.

Roddier D., Cermelli C., Aubault C. and Weinstein A. (2010) "WindFloat: A Floating foundation for Offshore Wind Turbines.Turbines." Journal of Renewable and Sustainable Energy No. 2 033104.

Vittori F., Bouchotrouch F., Lemmer F. and Azcona J. (2018) "Hybrid scaled testing of a 5MW floating wind turbine using the SiL method compared with numerical models", 37th International Conference on Ocean, Offshore and Arctic Engineering OMAE, Madrid, Spain.

Vittori F., Pires O., Azcona J., Uzunolgu E., Guedes-Soares C., Zamora-Rodríguez R. and Souto-Iglesias A., 2020, "Hybrid scaled testing of a 10MW TLP floating wind turbine using the SiL method to integrate the rotor thrust and moments", Developments in Renewable Energies Offshore, 1st Edition, Taylor & Francis Group, DOI: 10.1201/9781003134572-48.